

# MEASUREMENTS OF THE EFFECT OF COLLISIONS ON TRANSVERSE BEAM HALO DIFFUSION IN THE TEVATRON AND IN THE LHC

G. Stancari\*, G. Annala, T.R. Johnson, V. Previtali, D. Still, A. Valishev  
Fermi National Accelerator Laboratory, Batavia, IL, USA

R.W. Assmann†, Deutsches Elektronen-Synchrotron, Hamburg, Germany

R. Bruce, F. Burkart, S. Redaelli, B. Salvachua, G. Valentino, CERN, Geneva, Switzerland

## Abstract

Beam–beam forces and collision optics can strongly affect beam lifetime, dynamic aperture, and halo formation in particle colliders. Extensive analytical and numerical simulations are carried out in the design and operational stages of a machine to quantify these effects, but experimental data are scarce. The technique of small-step collimator scans was applied to the Fermilab Tevatron collider and to the CERN Large Hadron Collider to study the effect of collisions on transverse beam halo dynamics. We describe the technique and present a summary of the first results on the dependence of the halo diffusion coefficient on betatron amplitude in the Tevatron and in the LHC.

## INTRODUCTION

Beam quality and machine performance in circular accelerators depend on global quantities such as beam lifetimes, emittance growth rates, dynamic apertures, and collimation efficiencies. Calculations of these quantities are routinely performed in the design stage of all major accelerators, providing the foundation for the choice of operational machine parameters.

At the microscopic level, the dynamics of particles in an accelerator can be quite complex. Deviation from linear dynamics can be large, especially in the beam halo. Lattice resonances and nonlinearities, coupling, intrabeam and beam-gas scattering, and the beam–beam force in colliders all contribute to the topology of the particles' phase space, which in general includes regular areas with resonant islands and chaotic regions. In addition, various noise sources are present in a real machine, such as ground motion (resulting in orbit and tune jitter) and ripple in the radio-frequency and magnet power supplies. As a result, the macroscopic motion can in some cases acquire a stochastic character, describable in terms of diffusion [1–7].

In studies for the Superconducting Super Collider [8], the concept of diffusive dynamic aperture was discussed, as well as how it is affected by beam–beam forces, lattice nonlinearities, and tune jitter. Detailed theoretical studies of beam–beam effects and particle diffusion can be found, for instance, in Refs. [4–6, 9, 10]. In Ref. [7], the effects of random fluctuations in tunes, collision offsets, and beam

sizes were studied. Numerical estimates of diffusion in the Tevatron are given in Refs. [11–13].

Two main considerations lead to the hypothesis that macroscopic motion in a real machine, especially in the halo, may have a stochastic nature: (1) the superposition of the multitude of dynamical effects (some of which are stochastic) acting on the beam; (2) the operational experience during collimator setup, which generates spikes and dips in loss rates that often decay in time as  $1/\sqrt{t}$ , a typically diffusive behaviour.

It was shown that beam halo diffusion can be measured by observing the time evolution of particle losses during a collimator scan [14]. These phenomena were used to estimate the diffusion rate in the beam halo in the SPS and Sp $\bar{p}$ S at CERN [15–17], in HERA at DESY [14], and in RHIC at BNL [18]. An extensive experimental campaign was carried out at the Tevatron in 2011 [19] to characterize the beam dynamics of colliding beams and to study the effects of the novel hollow electron beam collimator concept [20]. Recently, the technique has also been used to measure halo diffusion rates in the LHC at CERN [21]. These measurements shed light on the relationship between halo population and dynamics, emittance growth, beam lifetime, and collimation efficiency. They are also important inputs for collimator system design and upgrades, including new methods such as channelling in bent crystals or hollow electron lenses.

Halo diffusion rates have been measured under various experimental conditions. In this paper, we focus on the comparison between colliding and separated beams, in an attempt to expose the effects of beam–beam forces. After briefly describing the method of small-step collimator scans, we present data on the dependence of the transverse beam halo diffusion coefficient on betatron amplitude in the Tevatron and in the LHC.

## EXPERIMENTAL METHOD

A schematic diagram of the apparatus is shown in Fig. 1 (top). All collimators except one are retracted. As the collimator jaw of interest is moved in small steps (inward or outward), the local shower rates are recorded as a function of time. Collimator jaws define the machine aperture. If they are moved towards the beam centre in small steps, typical spikes in the local shower rate are observed, which approach a new steady-state level with a characteristic relaxation time (Fig. 1, bottom). When collimators are retracted,

\* stancari@fnal.gov

† Previously at CERN, Geneva, Switzerland.

on the other hand, a dip in loss rates is observed, which also tends to a new equilibrium level. By using the diffusion model presented below, the time evolution of losses can be related to the diffusion rate at the collimator position. By independently calibrating the loss monitors against the number of lost particles, halo populations and collimation efficiencies can also be estimated. With this technique, the diffusion rate can be measured over a wide range of amplitudes. At large amplitudes, the method is limited by the vanishing beam population and by the fast diffusion times. The limit at small amplitudes is given by the level of tolerable loss spikes.

## MODEL

A diffusion model of the time evolution of loss rates caused by a step in collimator position was developed [22]. It builds upon the model of Ref. [14] and its assumptions of (1) constant diffusion rate, and (2) linear halo tails within the range of the step. These hypotheses allow one to obtain analytical expressions for the solutions of the diffusion equation and for the corresponding loss rates versus time. The present model addresses some of the limitations of the previous model and expands it in the following ways: (a) losses before, during, and after the step are predicted; (b) different steady-state rates before and after are explained; (c) determination of the model parameters

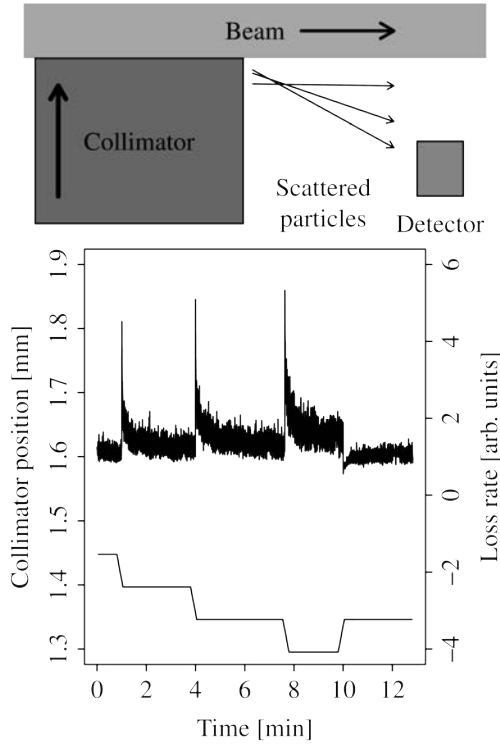


Figure 1: Schematic diagram of the apparatus (top), and an example of the response of local loss rates to inward and outward collimator steps (bottom).

(diffusion coefficient, tail population gradient, detector calibration, and background rate) is more robust and precise.

Following Ref. [14], we consider the evolution in time  $t$  of a beam of particles with phase-space density  $f(J,t)$ , described by the diffusion equation  $\partial_t f = \partial_J (D \partial_J f)$ , where  $J$  is the Hamiltonian action and  $D$  the diffusion coefficient in action space. The particle flux at a given location  $J = J'$  is  $\phi = -D \cdot [\partial_J f]_{J=J'}$ . During a collimator step, the action  $J_c = x_c^2 / (2\beta_c)$ , corresponding to the collimator half-gap  $x_c$  at a ring location where the amplitude function is  $\beta_c$ , changes from its initial value  $J_{ci}$  to its final value  $J_{cf}$  in a time  $\Delta t$ . The step in action is  $\Delta J \equiv J_{cf} - J_{ci}$ . In the Tevatron, typical steps in half-gap were  $50 \mu\text{m}$  in 40 ms; smaller steps ( $10 \mu\text{m}$  in 5 ms, typically) were possible in the LHC. In both cases, the amplitude function was of the order of a hundred metres. It is assumed that the collimator steps are small enough so that the diffusion coefficient can be treated as a constant in that region. If  $D$  is constant, the local diffusion equation becomes  $\partial_t f = D \partial_J^2 f$ . With these definitions, the particle loss rate at the collimator is equal to the flux at that location:

$$L = -D \cdot [\partial_J f]_{J=J_c}. \quad (1)$$

Particle showers caused by the loss of beam are measured with scintillator counters or ionization chambers placed close to the collimator jaw. The observed shower rate is parametrized as

$$S = kL + B, \quad (2)$$

where  $k$  is a calibration constant including detector acceptance and efficiency and  $B$  is a background term which includes, for instance, the effect of residual activation. Under the hypotheses described above, the diffusion equation can be solved analytically using the method of Green's functions, subject to the boundary condition of vanishing density at the collimator and beyond. Details are given in Ref. [22].

Local losses are proportional to the gradient of the distribution function at the collimator. The gradients differ in the two cases of inward and outward step, denoted by the I and O subscripts, respectively:

$$\begin{aligned} \partial_J f_I(J_c, t) &= -A_i + 2(A_i - A_c) P\left(\frac{-J_c}{w}\right) + \\ &\quad \frac{2}{\sqrt{2\pi}w} \left\{ -A_i(J_{ci} - J_c) + (A_i J_{ci} - A_c J_c) e^{-(J_c/w)^2/2} \right\} \\ \partial_J f_O(J_c, t) &= -2A_i P\left(\frac{J_{ci} - J_c}{w}\right) + 2(A_i - A_c) P\left(\frac{-J_c}{w}\right) + \\ &\quad \frac{2}{\sqrt{2\pi}w} (A_i J_{ci} - A_c J_c) e^{-(J_c/w)^2/2}. \end{aligned} \quad (3)$$

$$(4)$$

The positive parameters  $A_i = -[\partial_J f]_{J=J_{ci}}$  and  $A_f = -[\partial_J f]_{J=J_{cf}}$  are the opposites of the slopes of the distribution function before and after the step, whereas  $A_c$  varies linearly between  $A_i$  and  $A_f$  as the collimator moves. The parameter  $w$  is defined as  $w \equiv \sqrt{2Dt}$ . The function  $P(x)$

is the S-shaped cumulative Gaussian distribution function, such that  $P(-\infty) = 0$ ,  $P(0) = 1/2$ , and  $P(\infty) = 1$ .

The above expressions, Eqs. (3) and (4), are used to model the measured shower rates. Parameters are estimated from a fit to the experimental data. The background  $B$  is measured before and after the scan when the jaws are retracted. The calibration factor  $k$  is in general a function of collimator position, and can be determined independently by comparing the local loss rate with the number of lost particles measured by the beam current transformer. The fit parameters ( $kDA_i$ ) and ( $kDA_f$ ) are the steady-state loss rate levels before and after the step. The diffusion coefficient  $D$  depends on the measured relaxation time and on the value of the peak (or dip) in loss rates.

The model explains the data very well when the diffusion time is long compared to the duration of the step. The model can be extended by including a separate drift term (from the Fokker–Planck equation) or a non-vanishing beam distribution at the collimator.

## RESULTS

All Tevatron scans were done vertically on antiprotons, either at the end of regular collider stores (0.98 TeV per beam) or with only antiprotons in the machine at the same top energy. Losses were measured with scintillator paddles located near the collimators. (A detailed description of the Tevatron collimation system can be found in Ref. [23].)

The LHC measurements were taken in a special machine study at 4 TeV with only one bunch per beam, first with separated beams and then in collision, with vertical crossing at the first interaction point (IP1) and horizontal cross-

ing at IP5 [21]. Losses were measured with ionization chambers. Because of the negligible cross-talk between loss monitors, it was possible to simultaneously scrape proton beam 1 vertically and proton beam 2 horizontally.

Figure 2 shows a comparison of vertical beam halo diffusion measurements in the Tevatron and in the LHC, for inward collimator steps. To account for the different kinetic energies of the two machines, diffusion coefficients are plotted as a function of normalized vertical collimator action  $I \equiv \gamma_r J$ , where  $\gamma_r$  is the relativistic Lorentz factor. On the vertical axis, we plot the diffusion coefficient in normalized action space  $D_I \equiv \gamma_r^2 D$ , which stems from recasting the diffusion equation as follows:  $\partial_t f = \partial_J (D \partial_J f) \rightarrow \partial_t f = \partial_I (D_I \partial_I f)$ .

The dark-blue filled circles refer to the end of Tevatron collider Store 8733 (13 May 2011). The light-blue data (empty circles) were taken during a special antiproton-only fill (Store 8764, 24 May 2011). The LHC data were taken on 22 June 2012 and refer to beam 1 (vertical) with separated beams (empty red squares) and in collision (filled orange squares). The continuous lines represent the diffusion coefficients derived from the measured core geometrical emittance growth rates  $\dot{\epsilon}$ :  $D = \dot{\epsilon} \cdot J$ . (In this particular dataset, the synchrotron-light measurements were not sufficient for estimating emittance growth rates of colliding beams in the LHC.)

In the LHC, separated beams exhibited a slow halo diffusion, comparable with the emittance growth from the core. This fact can be interpreted as a confirmation of the extremely good quality of the magnetic fields in the machine. Collisions enhanced halo diffusion in the vertical plane by about one to two orders of magnitude. No significant diffusion enhancement was observed in the horizontal plane. The reason for this difference is not understood. In the Tevatron, the comparison between halo and core diffusion rates suggests that single-beam diffusion at these large amplitudes is dominated by effects other than residual-gas scattering and intrabeam scattering, pointing towards field nonlinearities and noise (including tune modulation generated by power-supply ripple). At the end of the store, collisions enhance diffusion by about one order of magnitude.

From the measured diffusion coefficients, estimates of impact parameters on the primary collimator jaws are possible [14]. One can also calculate the particle survival time versus the amplitude. The diffusion coefficient is related to the steady-state density of the beam tails, which can therefore be deduced by using a procedure that is complementary to the conventional static model, based on counting the number of lost particles at each collimator step. These and other consequences of beam halo diffusivity will be investigated in separate reports.

## CONCLUSIONS

The technique of small-step collimator scans was applied to the Fermilab Tevatron collider and to CERN's Large Hadron Collider to study transverse beam halo dynamics in relation to beam–beam effects and collimation.

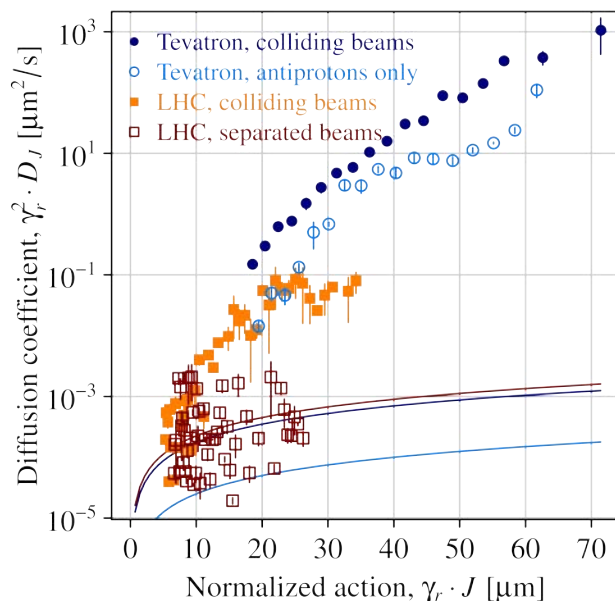


Figure 2: Measurements of vertical halo diffusion in the Tevatron and in the LHC.

We presented the first data on the dependence of transverse beam halo diffusion rates on betatron amplitude. In the Tevatron, vertical antiproton diffusion at the end of a collider store was compared with a special store with only antiprotons in the machine. Even with a reduced beam–beam force, the effect of collisions was dominant. A comparison with core emittance growth indicated that halo diffusion of single beams was driven by nonlinearities and noise, not by residual-gas or intrabeam scattering. In the LHC, horizontal and vertical collimator scans were performed during a special machine study with only one bunch per beam (i.e. no long-range beam–beam interactions). With separated beams, no significant difference was observed between halo and core diffusion, which indicated very low noise levels and nonlinearities. In collision, horizontal diffusion was practically unchanged; the vertical diffusion rate enhancement was a function of action and reached about two orders of magnitude. In general, it was confirmed that collimator scans are a sensitive tool for the study of halo dynamics as a function of transverse betatron amplitude.

### ACKNOWLEDGMENTS

The authors thank X. Buffat, R. De Maria, W. Herr, B. Holzer, T. Pieloni, J. Wenninger (CERN), H.J. Kim, N. Mokhov, T. Sen, and V. Shiltsev (Fermilab) for valuable discussions and insights. These measurements would not have been possible without the support of the CERN Operations Group and the Fermilab Accelerator Division personnel. In particular, we would like to thank S. Cettour Cave, A. Macpherson, D. Jacquet, M. Solfaroli Camillocci (CERN), M. Convery, C. Gattuso, and R. Moore (Fermilab).

Fermilab is operated by Fermi Research Alliance, LLC, under contract no. DE-AC02-07CH11359 with the United States Department of Energy. This work was partially supported by the US LHC Accelerator Research Program (LARP).

### REFERENCES

- [1] A.J. Lichtenberg and M.A. Lieberman, *Regular and Chaotic Dynamics* (New York: Springer, 1992).
- [2] T. Chen et al., Phys. Rev. Lett. 68 (1992) 33.
- [3] A. Gerasimov, Report No. FERMILAB-PUB-92-185 (1992).
- [4] F. Zimmermann, PhD Thesis, Hamburg University, Germany, Report No. DESY-93-059 (1993).
- [5] O.S. Brüning, PhD Thesis, Hamburg University, Germany, Report No. DESY-94-085 (1994).
- [6] F. Zimmermann, Part. Accel. 49 (1995) 67; Report No. SLAC-PUB-6634 (October 1994).
- [7] T. Sen and J.A. Ellison, Phys. Rev. Lett. 77 (1996) 1051.
- [8] J. Irwin, Report No. SSC-233 (1989).
- [9] Y. Papaphilippou and F. Zimmermann, Phys. Rev. ST Accel. Beams 2 (1999) 104001.
- [10] Y. Papaphilippou and F. Zimmermann, Phys. Rev. ST Accel. Beams 5 (2002) 074001.
- [11] T. Sen et al., Phys. Rev. ST Accel. Beams 7 (2004) 041001.
- [12] E.G. Stern et al., Phys. Rev. ST Accel. Beams 13 (2010) 024401.
- [13] V. Previtalli et al., Proc. 2012 Int. Particle Accelerator Conf. (IPAC12), New Orleans, Louisiana, USA, 20–25 May 2012, p. 1113.
- [14] K.-H. Mess and M. Seidel, Nucl. Instrum. Methods Phys. Res. A 351 (1994) 279; M. Seidel, PhD Thesis, Hamburg University, Report No. DESY-94-103 (June 1994).
- [15] L. Burnod, G. Ferioli, and J.B. Jeanneret, Report No. CERN-SL-90-01 (1990).
- [16] M. Meddahi, PhD Thesis, Université de Paris VII, France, Report No. CERN-SL-91-30-BI (1991).
- [17] W. Fischer, M. Giovannozzi, and F. Schmidt, Phys. Rev. E 55 (1997) 3507.
- [18] R.P. Fliller III et al., Proc. 2003 Particle Accelerator Conf. (PAC03), Portland, Oregon, USA, 12–16 May 2003, p. 2904.
- [19] G. Stancari et al., Proc. 2011 Int. Particle Accelerator Conf. (IPAC11), San Sebastián, Spain, 4–9 September 2011, p. 1882.
- [20] G. Stancari et al., Phys. Rev. Lett. 107 (2011) 084802; arXiv:1105.3256 [phys.acc-ph].
- [21] G. Valentino et al., Phys. Rev. ST Accel. Beams 16 (2013) 021003.
- [22] G. Stancari, arXiv:1108.5010 [physics.acc-ph], Report No. FERMILAB-FN-0926-APC (2011).
- [23] N. Mokhov et al., J. Instrum. 6 (2011) T08005.